Iran Polym J (2016) 25:957–965
DOI 10.1007/s13726-016-0482-0

ORIGINAL PAPER

Bio-based shape memory epoxy resin synthesized from rosin acid

Tingting Li[1,2] · Xiaoqing Liu[1] · Yanhua Jiang[1] · Songqi Ma[1] · Jin Zhu[1]

Received: 7 June 2016 / Accepted: 26 September 2016 / Published online: 5 October 2016

Abstract A bio-based shape memory epoxy resin (DGEAPA) was synthesized from rosin to achieve the sustainability of shape memory epoxy resin, and its chemical structure was determined by FTIR and ^{1}H NMR. For comparison, a petroleum-based epoxy, diglycidyl ester of terephthalic acid (DGT) having one benzene ring, was also synthesized. The properties, including thermal and mechanical properties, as well as shape memory properties of the epoxy resins cured with poly(propylene glycol)-bis (2-aminopropyl ether) (D230), were studied by differential scanning calorimeter, dynamic mechanical analysis, thermogravimetric analysis, tensile test, and U-type shape memory test. The effect of the stoichiometric ratio n_{DGEAPA}/n_{DGT} on the properties was studied as well. The thermal and mechanical properties, including thermal stability, glass transition temperature, tensile strength, and modulus of the cured epoxy systems, were found to be increased with DGEAPA incremental content, and the cured neat rosin-based epoxy system exhibited the highest properties. Both the cured rosin-based epoxy and the cured DGEAPA showed significant shape memory performance. Meanwhile, the rosin ring structure made the cured rosin-based epoxy systems display excellent shape recovery fixity, while small lower shape recovery and shape recovery rate relative to the cured neat DGT system. Therefore, the rosin-based epoxy resin has a great potential in the shape memory material applications.

Keywords Bio-based epoxy resin · Sustainability · Hydrophenanthrene ring · Rosin acid · Shape memory

✉ Xiaoqing Liu
liuxq@nimte.ac.cn

✉ Songqi Ma
masongqi@nimte.ac.cn

[1] Ningbo Institute of Materials Technology and Engineering, Chinese Academy of Sciences, Ningbo, Zhejiang 315201, People's Republic of China

[2] Nano Science and Technology Institute, University of Science and Technology of China, Suzhou 215123, People's Republic of China

Introduction

Shape memory polymers (SMPs) represent a class of smart polymer materials that can memorize temporary shapes and recover their permanent shapes with respect to external stimuli [1–3]. These include thermoplastic [4–6] and thermosetting types of SMPs [7]. Compared with thermoplastic SMPs, thermosetting types have some advantages by greater thermal and chemical stability [8], higher shape recovery stress, higher shape fixity ratio, and better processability. Thermosetting SMPs, especially epoxy resin, have wide application prospects, such as robot hand [9] and spacecrafts [10]. Diglycidyl ether of bisphenol A (DGEBA) represents the most reported epoxy precursors for shape memory epoxy resins in the world, while DGEBA is largely dependent on petroleum-based raw material, bisphenol A, which is deemed to be toxic to living organisms [11]. Therefore, sustainable epoxy resins with non-toxicity should be developed as alternatives for DGEBA.

Recent years have witnessed rapid developments in bio-based polymers. Up to now, a large quantity of renewable materials, such as starch [12], cellulose [13], chitosan [14], lignin [15], vegetable oil [16], and rosin acid [17, 18], have been employed to synthesize bio-based polymeric materials. Among which, rosin which contains more than 90 % rosin acids with rigid structure similar to petroleum-based cycloaliphatic or aromatic compounds is an abundantly

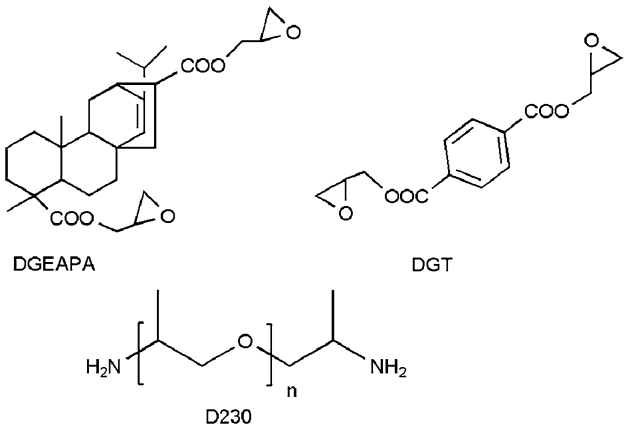

Scheme 1 Chemical structures of DGT, DGEAPA, and D230

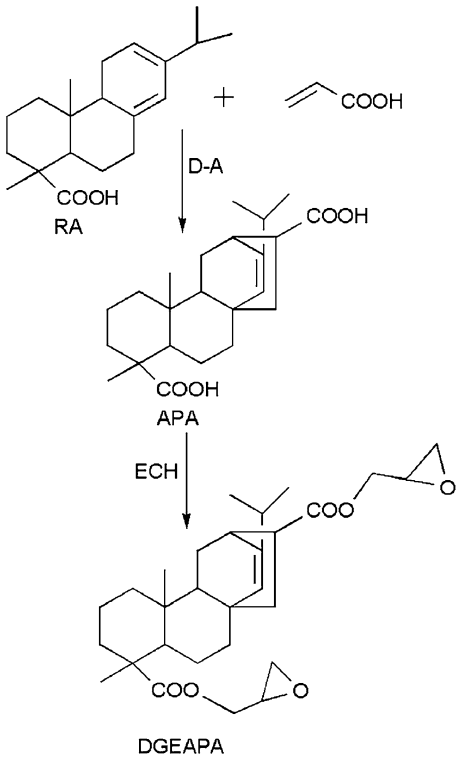

Scheme 2 Synthesis procedure of DGEAPA from RA

available natural product, with a global annual production of about 1.2 million tons [19]. Thus, many efforts are made to develop epoxy resins from rosin acids to acquire a suitable alternative to DGEBA [20–22], and our previous works proved that rosin-based epoxy and curing agents exhibit better or similar thermal and mechanical properties compared with their petroleum-based counterparts [23–25]. Moreover, rosin ring was demonstrated to have a significant influence on the shape memory properties of polymer in our previous work [26]. Rosin ring was incorporated into the main chain of polyurethanes, which resulted in excellent shape memory properties with recoverable strain of 960 %, nearly 2.5 times of the highest reported value (400 %), and shape recovery of 85 % [26].

In this paper, a rosin-based shape memory epoxy resin was synthesized. The study on the structure–property relationships was reported by tests on the epoxy monomer (DGEAPA, as shown in Scheme 1) other than rosin-based epoxy oligomers or mixtures [27–29]. For comparison, the petroleum-based counterpart containing planar benzene ring, diglycidyl ester of terephthalic acid, was also synthesized as the control. Following the syntheses, the epoxies were cured with poly(propylene glycol)-bis(2-aminopropyl ether) (D230), and their thermal and mechanical properties, especially the shape memory properties were systematically investigated. The results in this study might provide us new insight to develop the epoxy with good shape memory properties.

Experimental

Materials

Rosin acid (RA), acrylic acid (AA), benzyltriethylammonium chloride (TEBAC), cetyltrimethyl ammonium chloride (CTMAC), and poly(propylene glycol)-bis (2-aminopropyl ether) (D230) were purchased from Aladdin Reagent, China. Sodium hydroxide, petroleum ether, anhydrous ether, epichlorohydrin (ECH), dichloromethane, and terephthalic acid (TPA) were obtained from Sinopharm Chemical Reagent Co., China. All the chemicals were used as received.

Synthesis of acrylic pimaric acid (APA)

The reaction components included 15.1 g (0.05 mol) rosin acid, 4.4 g (0.06 mol) acrylic acid, and 0.1 g hydroquinone (as a polymerization inhibitor), which were added into a 250 mL three-necked flask equipped with a reflux condenser, a magnetic stirrer, and a N_2 stream. The mixture was heated at 140 °C for 0.5 h, 160 °C for 0.5 h, and 180 °C for another 9 h under the protection of nitrogen. After that, the gaseous unreacted acrylic acid was removed by N_2. Finally, the reaction was stopped and cooled to room temperature. The mixture was dissolved in anhydrous ether and precipitated in excess petroleum ether. The pale yellow precipitate was collected by filtration and washed three times with de-ionized water. The pale yellow crude product was recrystallized from acetone to obtain the pure APA which is a white, solid, and powder material weighing 10.5 g (yield: 56 %). The synthetic scheme is shown in Scheme 2.

^{1}H NMR (400 MHz, $CDCl_3$, δ ppm): 5.37 (s, H), 2.50 (s, H), 2.31 (m, 2H), and 0.5–2.0 (m, 28H). FTIR (cm^{-1}): 1162, 1276, 1459, 1693, 2869, and 2947.

Synthesis of diglycidyl ester of acrylic pimaric acid (DGEAPA)

The components, including 10.5 g (0.028 mol) APA, 69 g (0.75 mol) epichlorohydrin, and 0.0842 g benzyltriethylammonium chloride (TEBAC, as a phase transfer catalyst), were entered into a 100 mL three-necked round flask equipped with a reflux condenser and a magnetic stirrer. The mixture was stirred at 115 °C for 2 h. Then, the reaction was cooled to 60 °C, and 2.98 g (0.074 mol) sodium hydride and 4.200 g (0.074 mol) were added. After that, the reaction was continued at 60 °C for another 3 h. Finally, the mixture was cooled to room temperature and the solid precipitate was removed via filtration. The filtrate was diluted with 100 mL dichloromethane (CH_2Cl_2) and washed with 60 mL of de-ionized water three times. The CH_2Cl_2 layer was dried with anhydrous magnesium sulfate and concentrated using a rotary evaporator, giving 11.9 g (yield: 88 %) of yellowish liquid. The synthetic process is presented in Scheme 2.

^{1}H NMR (400 Hz, $CDCl_3$, δ ppm): 5.37 (s, H), 4.43 (d, H), 4.1 (t, H), 3.95 (m, H), 3.85 (m, H), 3.20 (m, 2H), 2.85 (m, 2H), 2.65 (m, 2H), 2.50 (s, H), 2.31 (m, 2H), and 0.5–2.0 (m, 28H). FTIR (cm^{-1}): 840, 910, 1146, 1273, 1460, 1726, 2870, and 2940.

Synthesis of diglycidyl ester of terephthalic acid (DGT)

The reaction components, including 30.2 g (0.18 mol) of terephthalic acid, 273 g (2.95 mol) of epichlorohydrin, and 1.51 g of cetyltrimethyl ammonium chloride (CTMAC, as a phase transfer catalyst), were put into a 500 mL three-necked flask equipped with a magnetic stirrer and a reflux condenser. The mixture was stirred at 90 °C for 3 h and then cooled to room temperature and 45 g aqueous solution of sodium hydroxide was added. Finally, the reaction was heated to 30 °C for 6 h. The mixture was washed with deionized water three times. The organic part was concentrated by a rotary evaporator. At the end, the white power weighing 39 g (yield: 77 %) was obtained. The synthetic route is presented in Scheme 3.

^{1}H NMR (400 Hz, $CDCl_3$, δ ppm): 8.15 (d, 4H), 4.71 (m, 2H), 4.20 (m, 2H), 3.39 (m, 2H), 2.92 (t, 2H), and 2.76 (m, 2H). FTIR (cm^{-1}): 824, 982, 1460, 1074, 1117, 1276, 1502, 1577, 1720, 2956, and 3064.

Preparation of cured epoxy resins

Epoxy monomers (DGEAPA or DGT) and poly(propylene glycol)-bis(2-aminopropyl ether) (D230) with the desired ratios are shown in Table 1. Epoxy monomer was cured with curing agent (D230) in a 1:1 equivalent ratio. An appropriate amount of CH_2Cl_2 was added to dissolve the curing agent and epoxy before it was stirred for 20 min at room temperature to form a homogeneous mixture. The mixture was transferred into a vacuum oven at 60 °C for 2 h to remove CH_2Cl_2 and then poured into a stainless steel mold to be cured at 100 °C for 2 h, 130 °C for 2 h, and 170 °C for 4 h. All the samples were cured under the same conditions and removed from the stainless steel mold for dynamic mechanical analysis, and thermal and mechanical property tests.

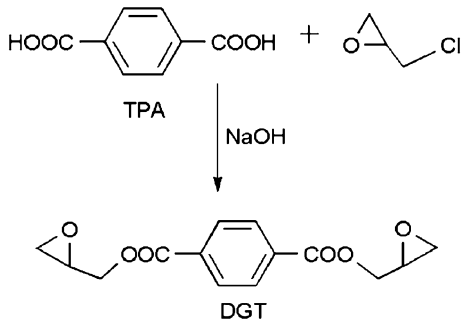

Scheme 3 Synthesis procedure of DGT from TPA

Table 1 Compositions for the different systems

Sample	DGEAPA (mol)	DGT (mol)	D230 (mol)	M_c
EP 0	0	1	0.5	785
EP0.5	0.5	0.5	0.5	1027
EP1	1	0	0.5	1274

Characterization

Fourier transform infrared (FTIR) spectra were recorded with Nicolet 6700 FTIR, scanning from 4000 to 400 cm^{-1}.

^{1}H NMR spectra were recorded with a Bruker 400 MHz Avance III spectrometer. It was conducted at room temperature with the solvent of deuterated chloroform ($CDCl_3$).

The differential scanning calorimetry (DSC) measurement was carried out using a Mettler-Toledo TGA/DSCI-under nitrogen atmosphere. The sample weighed about 7 mg and the test was conducted from 0 to 130 °C at a heating rate of 5 °C min^{-1}.

The thermogravimetric analyses (TGA)' measurement was performed on a Mettler-Toledo TGA/DSC1 thermogravimetric analyzer (Switzerland) under a nitrogen atmosphere at a scanning rate of 10 °C min^{-1} from 50 to 600 °C. Samples each weighing about 5 mg were used for the tests.

The mechanical properties of the cured epoxy resins were analyzed by Instron 5567 Universal Mechanical Testing Machine at a speed of 10 mm according to GB/T 1040.2-2006. Tensile tests at room temperature were carried out using dumbbell-shaped specimens with gauge length of 12 mm. For this test, at least five specimens were measured for each sample to obtain an average value.

DMA was performed on a Mettler-Toledo DMA/SDTA 861e using a tensile mode at a frequency of 1 Hz. The samples were scanned from 25 to 180 °C at a heating rate of 5 °C min^{-1}.

Rectangular specimens (75 × 7.1 × 1.6 mm^3) were applied to evaluate the shape memory properties of the cured epoxy resins. The shape memory test was carried out according to the following steps: (1) the specimens were heated to a certain temperature (T_g +30 °C); (2) the heated specimens were bent into "U shapes" and they were cooled down at room temperature for fixing the shape; (3) the U-shaped specimens were reheated to recover their original shapes at T_g +30 °C and the shape recovery process was observed. The maximum angle of bending was tested as θ_{max}. The initial deformation angle of the fixed sample was measured as angle θ_{fixed}. The deformation angle after recovering process was measured as angle θ_{final}.

The shape fixity (R_f) and shape recovery (R_r) were calculated using the following equations:

$$Rf = [\theta_{fixed}/\theta max] \times 100\ \% \quad (1)$$

$$Rr = [(\theta_{fixed} - \theta_{final})/\theta max] \times 100\ \%. \quad (2)$$

Results and discussion

Chemical characterization of DGEAPA and DGT

The chemical structures of DGT and DGEAPA were determined by FTIR and ^{1}H NMR. The FTIR spectra of APA, DGEAPA, and DGT are presented in Fig. 1. In the FTIR spectrum of DGT, the characteristic peaks arising from C–O stretching vibration and C=O stretching vibration appear at 1276 and 1720 cm^{-1}, respectively, the peaks at 2956 cm^{-1} belong to the stretching of C–H in oxirane ring, the peaks at 3060 and 1502 cm^{-1} correspond to the stretching absorptions of C–H and C=C in benzene ring, and the peaks at 1074, 1276, and 860 cm^{-1} belong to the C–O–C in oxirane ring. In the FTIR spectrum of APA, the peak at 1693 cm^{-1} represents the C=O stretching vibration of –COOH. After the reaction between APA and ECH, as shown in the FTIR spectrum of DGEAPA, ester bonds were formed which can be seen from the disappearance of the characteristic peak of C=O from –COOH and appearance of the peak at 1726 cm^{-1} corresponding to the stretching absorptions of C=O from ester bonds. Meanwhile, the

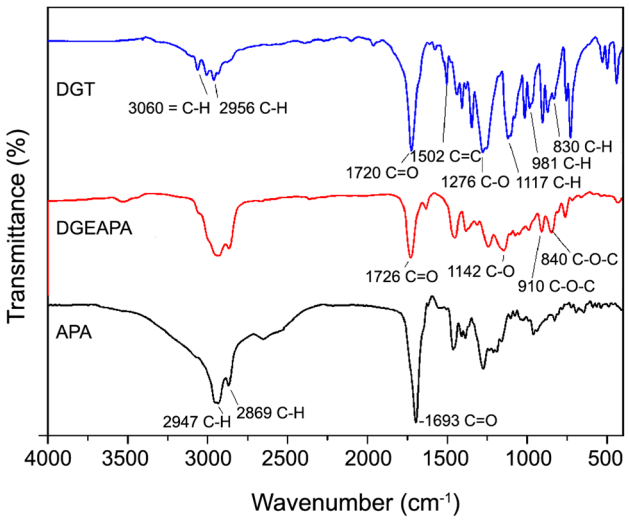

Fig. 1 FTIR spectra of APA, DGEAPA, and DGT

peaks at 910 and 840 cm^{-1} belong to the characteristic absorptions of oxirane ring.

To further identify their structures, the ^{1}H NMR spectra of APA, DGEAPA, and DGT are also shown in Fig. 2. The spectrum of DGT (Fig. 2a) exhibits the peaks of protons H_a, $H_{a'}$, H_b, H_e, H_f, and H_f of oxirane ring, the peaks of protons H_c, $H_{c'}$, H_d, and H_d, of CH_2 next to the oxirane ring, and the peak of protons H_g on the benzene ring. In the spectrum of APA (Fig. 2b), the peak at 5.4 ppm is ascribed to the proton H_b attached to the unsaturated carbon on the rosin ring, the peaks at 2.2–2.6 ppm represent the protons H_a, H_c, and H_d of CH next to the C=C bond on the rosin ring and H_d of CH next to –COOH. In the spectrum of DGEAPA (Fig. 2c), there appear characteristic peaks of protons H_a, $H_{a'}$, H_b, H_d, H_d, and H_e on oxirane ring at 2.6–2.7, 2.8–2.9, and 3.1–3.3 ppm, and the peaks for protons H_c, $H_{c'}$, H_f, and H_f of CH_2 next to oxirane ring at 3.8–4.5 ppm. In addition, the integrated area ratios of the characteristic signals for protons in each ^{1}H NMR spectra were all in good agreement with the theoretical values. These results indicate that the target epoxy monomers were successfully synthesized.

The cross-link density of the cured epoxy resins

The compositions of different epoxy systems are summarized in Table 1. The average molecular weights (M_c) can be used to reflect the cross-link density of the cured epoxy resins. The higher the M_c, the lower would be the cross-link density. The average molecular weights (M_c) between cross-link points of different samples (listed in Table 1) are calculated using the following equation [30]

$$Mc = (M_{DGEAPA} \times n_{DGEAPA} + M_{DGT} \times n_{DGT} + Md230 \times nd230)/nd230 \quad (3)$$

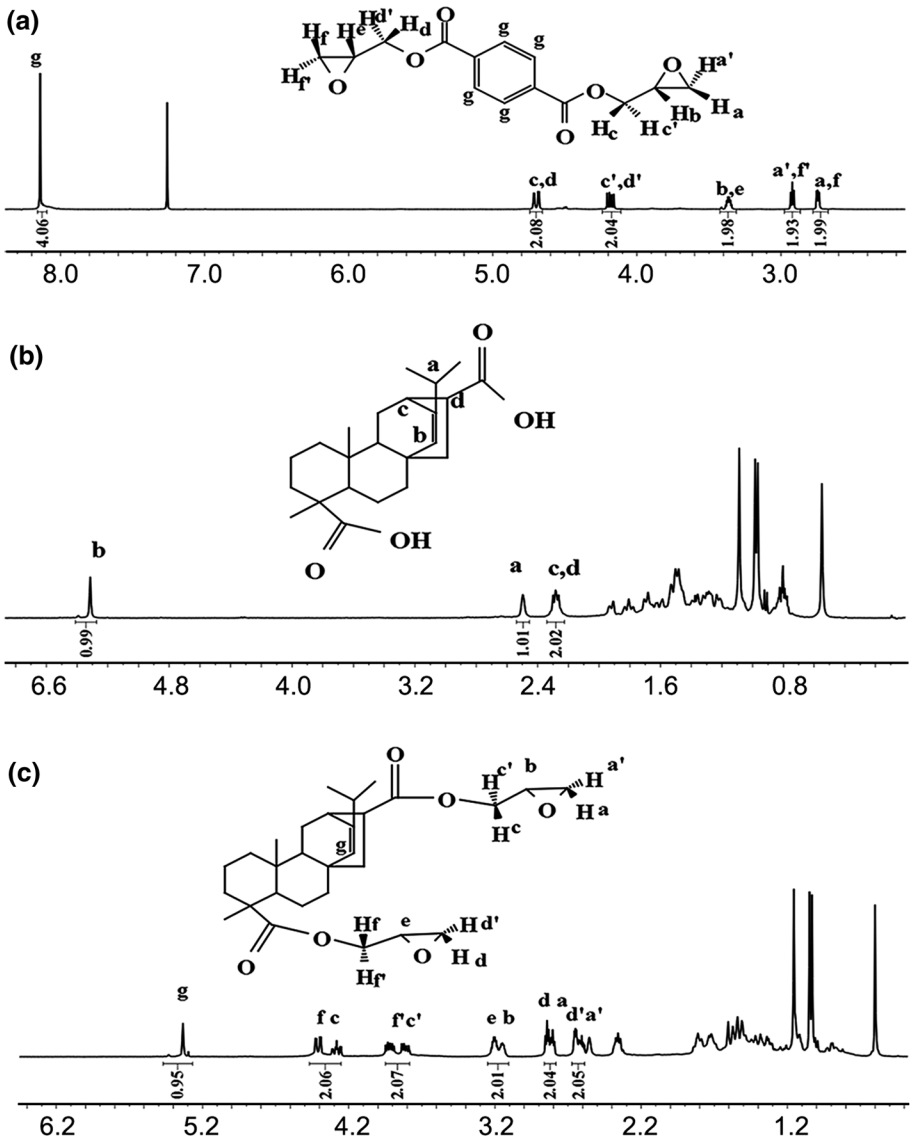

Fig. 2 ^{1}H NMR spectra of: **a** DGT, **b** APA, and **c** DGEAPA

where M and n represent the molar mass and molarity of the corresponding component in the epoxy systems, respectively. As seen from Table 1, the M_c values of the epoxy systems increase with the increase of DGEAPA content, since DGEAPA has molecular weight of 486 higher than that of DGT with a molecular weight of 278. This means that the cross-link density of the cured epoxy resins decreases with the incremental content of DGEAPA.

Mechanical properties of the cured epoxy resins

The tensile stress–strain curves for the cured epoxy resins are shown in Fig. 3 and the data for their tensile properties are listed in Table 2. Obviously, the stress of all cured epoxy systems presents linear increase with strain until final rupture without yielding. EP1 exhibits higher tensile strength and tensile modulus than EP0, and the tensile

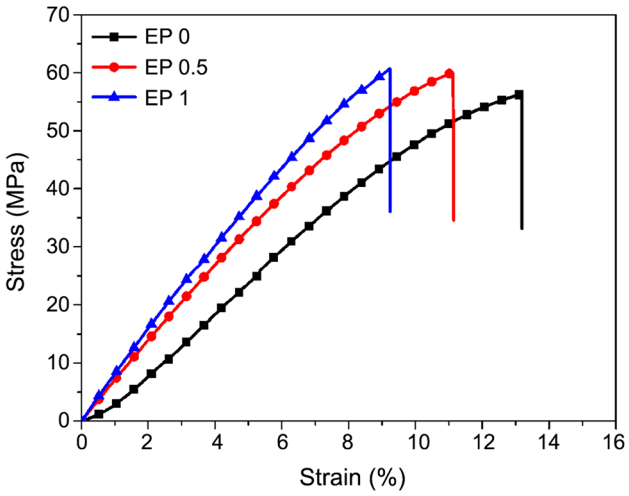

Fig. 3 Tensile curves for *different cured* epoxy resins

Table 2 Mechanical properties of the cured epoxy resins

Sample	Tensile strength (MPa)	Tensile modulus (MPa)	Elongation-at-break (%)
EP0	56 ± 2	511 ± 9	13.2 ± 0.6
EP0.5	61 ± 4	684 ± 26	11.1 ± 0.8
EP1	62 ± 2	779 ± 23	9.2 ± 0.9

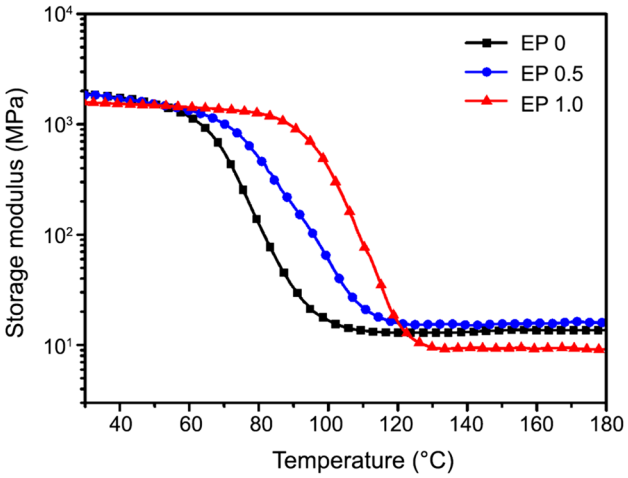

Fig. 4 *DMA curves* for epoxy series: storage versus temperature

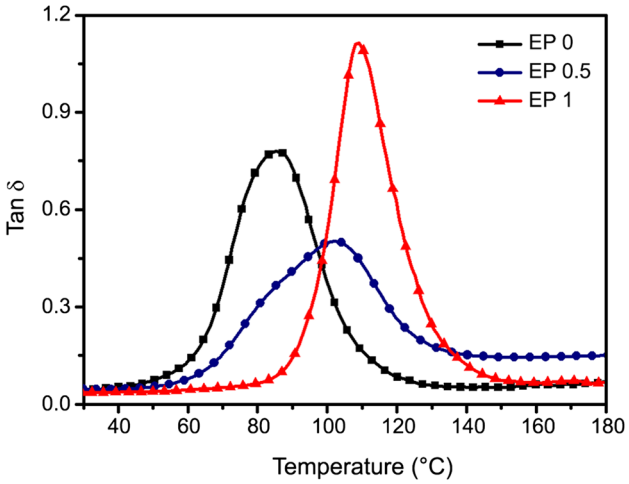

Fig. 5 *DMA curves* for epoxy series: tan delta versus temperature

strength and tensile modulus increase with the incremental content DGEAPA content. This might be due to the rigid rosin ring of DEEAPA. In general, a polymer which contains more rigid units are usually more brittle [31], and this may be interpreted to lower elongation-at-break of EP1 compared with EP0 and EP0.5.

Dynamic mechanical properties of the cured epoxy resins

The dynamic mechanical properties of the cured epoxies were investigated by DMA and the curves are shown in Figs. 4 and 5. All the samples showed relatively constant storage modulus in their respective glassy and rubbery regions and the difference between the glassy modulus and rubbery modulus for each individual sample has been in 2–3 orders of magnitude (Fig. 4). Figure 5 indicates the loss tangent (tan delta) for different samples as a function of temperature. The peak temperature of the tan delta curves was recorded as the glass transition temperature (T_g) of the cured samples, the data are shown in Table 3. Clearly, the T_g of the cured epoxy systems increased with the increasing content of DGEAPA. The T_g of cross-linked polymers has close ties with their cross-link density and the chain segment structure [32–34]. Theoretically, a higher cross-link density or more rigid chain segment will produce a higher T_g. The neat DGEAPA system (EP 1) has lower cross-link density but has much more rigid chain segment

Table 3 Thermal properties of the cured epoxy resins

Sample	T_g (°C)		T_{d5} in N_2 (°C)	T_{d50} in N_2 (°C)
	DMA	DSC		
EP0	85	92	272	351
EP0.5	102	105	282	368
EP1	110	115	317	381

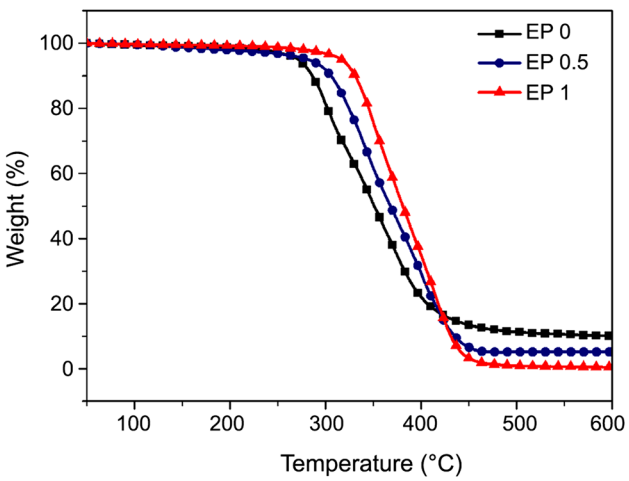

Fig. 6 *TGA curves* of cured systems

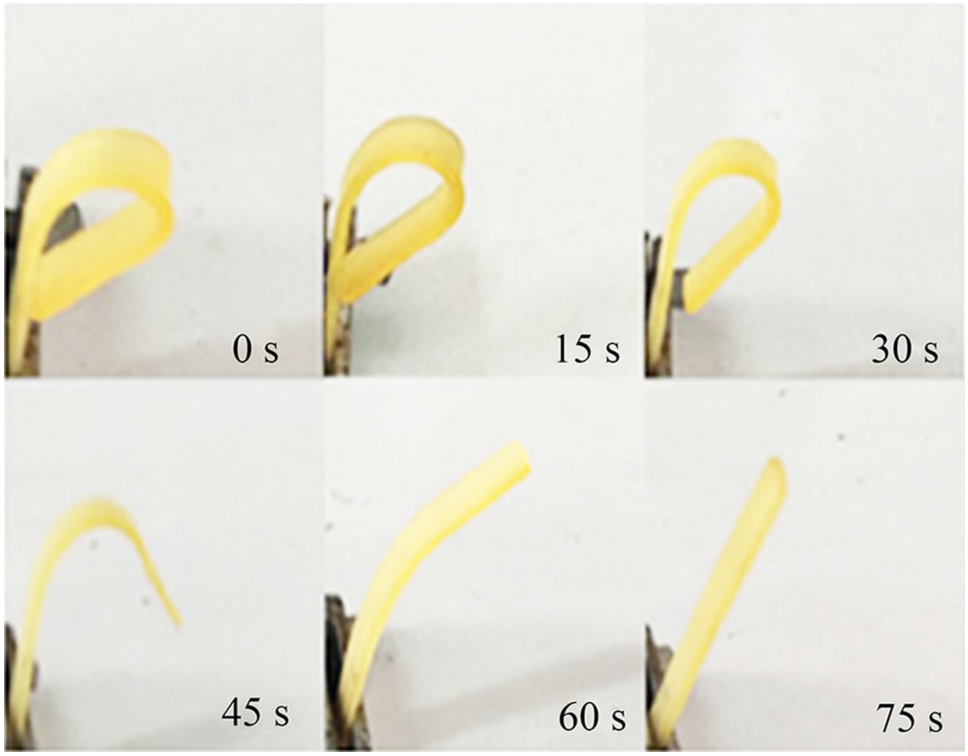

Fig. 7 Shape recovery process of sample EP1 in a 145 °C oven

Table 4 Shape fixity, shape recovery, and shape recovery time of the cured epoxy resins

Sample	Shape fixity R_f (%)	Shape recovery R_r (%)	Shape recovery time t (s)
EP0	98.6	98.3	104
EP0.5	99.0	97.2	147
EP1	99.4	96.9	155

structure (rosin ring) than the neat DGT system (EP 0). By introducing DGEAPA, the impact of greater chain rigidity of the cross-linked networks on T_g exceeds the impact of lowered cross-link density, corresponding to the increasing T_g of cross-linked networks with the increase in DGEAPA content. The same trend in T_g values was obtained by DSC measurement, as shown in Table 3.

Thermal degradation behavior of the cured epoxy resins

The thermal stability and degradation behaviors of the cured epoxies were investigated by TGA. The TGA curves are shown in Fig. 6. The values of the initial degradation temperature for 5 % weight loss (T_{d5}) and 50 % weight loss (T_{d50}) are listed in Table 3. The neat DGEAPA system (EP1) exhibits higher T_{d5} and T_{d50} than the neat DGT system (EP0), and the T_{d5} and T_{d50} of the cured epoxy systems increased with the increasing content of DGEAPA. These results meant that the DGEAPA systems show higher thermal stability than DGT system. This might be due to the more rigid rosin ring of DGEAPA than benzene ring of DGT, which could be reflected from the higher modulus of DGEAPA systems than the neat DGT system [35–37].

Shape memory properties

The samples were tested at T_g + 30 °C using the U-type shape memory test (the T_g values were obtained from DSC). Figure 7 shows a series of photographs of the shape recovery process of EP1 (55 × 5 × 1 mm) in a 145 °C oven. Using only 75 s, bended EP1 could almost recover to the original shape. Table 4 presents the data for the shape memory properties of the cured samples from the U-type shape memory test. As can be seen, all the samples show high shape fixed ratio (R_f) and recovery ratio (R_r). The R_f of the cured samples increased with the increase of DGEAPA content and the neat DGEAPA system shows the highest R_f (99.4 %). While the R_r and shape recovery rate of the cured samples decreased with the increase of DGEAPA content. These might be due to the steric hindrance of the rosin ring structure. The steric hindrance of rosin ring structure resulted in the lower chain mobility of DGEAPA systems than the neat DGT system [38], corresponding to the higher shape fixity and slower shape recovery of DGEAPA systems than the neat DGT system. Figures 8 and 9 show the

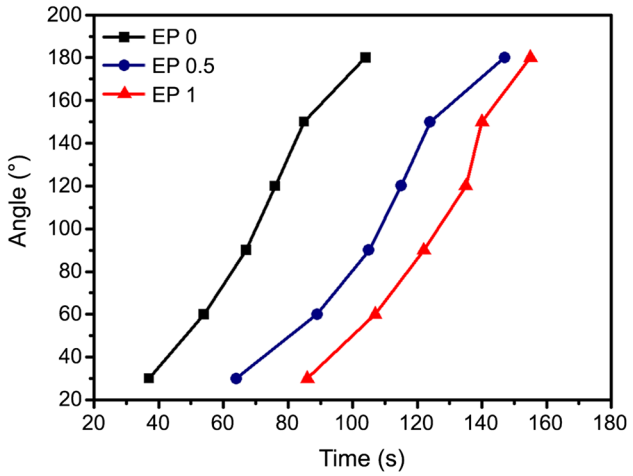

Fig. 8 Shape recovery time of the *cured epoxy resins* as a function of shape recovery angle

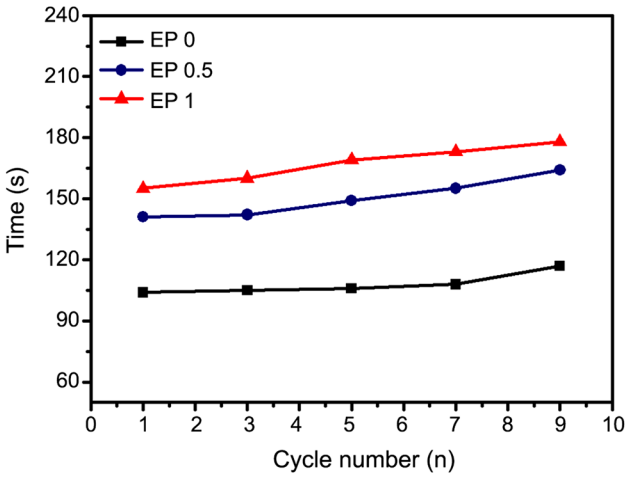

Fig. 9 Shape recovery time of the *cured epoxy resins* as a function of the number of shape memory cycle

relationships between recovery time and recovery angle and the number of shape memory cycle of the shape memory epoxy series at $T_g + 30$ °C. As can be seen from Fig. 8, the recovery rate decreased at the last stage from 150° to 180°. This can be explained by the reason that the main stored strain energy has already been released at the earlier stages, resulting in the relatively slow recovery rate of the cured samples at the last stage [39]. After the cyclic U-type shape memory test, the shape recovery rate of all the cured samples reduced a little bit, as shown in Fig. 9.

Conclusion

A rosin-based epoxy monomer DGEAPA and its petroleum-based counterpart containing benzene ring DGT (as the control) were successfully synthesized. The cured rosin-based epoxy exhibited higher thermal and mechanical properties, including glass transition temperature, thermal stability, tensile strength, and modulus. Both the cured DGEAPA and DGT showed great shape memory performance. Meanwhile, the steric rosin ring structure made the cured DGEAPA systems own excellent shape recovery fixity, while a bit lower shape recovery and shape recovery rate than the cured DGT systems. Thus, the rosin-based epoxy resin has a great potential to be used as shape memory material and the non-planar rosin ring structure could be used to regulate the shape memory properties of epoxy resins.

Acknowledgments The authors acknowledge financial support from Projects 51473180 and 51373194 supported by the National Natural Science Foundation of China, and Project 2012229 from Youth Innovation Promotion Association of the Chinese Academy of Sciences.

References

1. Yasar RM, Marc B, Karl K, Andreas L (2013) Multifunctional hybrid nanocomposites with magnetically controlled reversible shape-memory effect. Adv Mater 25:5730–5733
2. Ariraman M (2015) Shape memory effect on the formation of oxazoline and triazine rings of BCC/DGEBA copolymer. RSC Adv 5:69720–69727
3. Lendlein A, Jiang HY, Junger O, Langer R (2005) Light-induced shape-memory polymers. Nature 434:879–882
4. Ping P, Wang WS, Chen XS, Jing XB (2005) Poly(epsilon-caprolactone) polyurethane and its shape-memory property. Biomacromolecules 6:587–592
5. Dolog R, Weiss RA (2013) Shape memory behavior of a polyethylene-based carboxylate ionomer. Macromolecules 46:7845–7852
6. Gu L, Cui B, Wu Q, Yu H (2016) Bio-based polyurethanes with shape memory behavior at body temperature: effect of different chain extenders. RSC Adv 6:17888–17895
7. Kumar KSS, Nair CPR (2014) Hydrophobic shape memory poly(oxazolidone-triazine) cyclomatrix networks with high transition temperatures. RSC Adv 4:2969–2973
8. Rousseau IA (2008) Challenges of shape memory polymers: a review of the progress toward overcoming SMP's limitations. Polym Eng Sci 48:2075–2089
9. Wu Y, Hu J, Zhang C, Han J, Wang Y, Kumar B (2015) A facile approach to fabricate a UV/heat dual-responsive triple shape memory polymer. J Mater Chem A 3:97–100
10. Liu Y, Du H, Liu L, Leng J (2014) Shape memory polymers and their composites in aerospace applications: a review. Smart Mater Struct 23:23001–23022
11. Flint S, Markle T, Thompson S, Wallace E (2012) Bisphenol A exposure, effects, and policy: a wildlife perspective. J Environ Manage 104:19–34
12. Coativy G, Gautier N, Pontoire B, Buleon A, Lourdin D, Leroy E (2015) Shape memory starch-clay bionanocomposites. Carbohydr Polym 116:307–313
13. Oun AA, Rhim JW (2014) Preparation and characterization of sodium carboxymethyl cellulose/cotton linter cellulose nanofibril composite films. Carbohydr Polym 127:101–109
14. Badgujar KC, Bhanage BM (2015) Immobilization of lipase on biocompatible copolymer of polyvinyl alcohol and chitosan

for synthesis of laurate compounds in supercritical carbon dioxide using response surface methodology. Proc Biochem 50:1224–1236
15. Azhar NA, Soloi S, Majid RA, Jamaluddin J (2015) Grafting efficiency of lignin-grafted-polyacrylic acid. Appl Mech Mater 735:182–185
16. Lligadas G, Ronda JC, Galia M, Cadiz V (2013) Monomers and polymers from plant oils via click chemistry reactions. J Polym Sci Part A Polym Chem 51:2111–2124
17. Ma Q, Liu X, Zhang R, Zhu J, Jiang Y (2013) Synthesis and properties of full bio-based thermosetting resins from rosin acid and soybean oil: the role of rosin acid derivatives. Green Chem 15:1300–1310
18. Zhu YZ, Zhang SZ, Geng ZM, Wang DY, Liu F, Zhang MH, Bian H, Xu WM (2014) Simultaneous determination of abietic acid and dehydroabietic acid residues in duck meat by HPLC-PAD-FLD. Food Anal Meth 7:1627–1633
19. Ma S, Li T, Liu X, Zhu J (2016) Research progress on bio-based thermosetting resins. Polym Int 65:164–173
20. Atta AM, Mansour R, Abdou MI, Sayed AM (2004) Epoxy resins from rosin acids: synthesis and characterization. J Hazard Mater 15:514–522
21. Brocas AL, Llevot A, Mantzaridis C, Cendejas G, Caillol S, Carlotti S, Cramail H (2014) Epoxidized rosin acids as co-precursors for epoxy resins. Des Monomers Polym 17:301–310
22. Qin J, Liu H, Zhang P, Wolcott M, Zhang J (2014) Use of eugenol and rosin as feedstocks for biobased epoxy resins and study of curing and performance properties. Polym Int 63:760–765
23. Li C, Liu X, Zhu J, Zhang C, Guo J (2013) Synthesis, characterization of a rosin-based epoxy monomer and its comparison with a petroleum-based counterpart. J Macromol Sci A 50:321–329
24. Liu XQ, Huang W, Jiang YH, Zhu J, Zhang CZ (2012) Preparation of a bio-based epoxy with comparable properties to those of petroleum-based counterparts. Express Polym Lett 6:293–298
25. Liu X, Zhang J (2010) High-performance biobased epoxy derived from rosin. Polym Int 59:607–609
26. Zhang L, Jiang Y, Xiong Z, Liu X, Na H, Zhang R, Zhu J (2013) Highly recoverable rosin-based shape memory polyurethanes. J Mater Chem A 1:3263–3267
27. Xia JL, Shang S, Xie H, Huang H, Wang DX (2002) Study on curing reaction and properties of the acrylic modified rosin based epoxy resin. Thermoset Resin 17:1–5
28. Deng L, Shen M, Gan L, Yu J, Ha C (2011) Properties of epoxy resins based on acrylic acid rosin with different flexible chains. Polym Mater Sci Eng 27:106–108
29. Atta AM, Mansour R, Abdou MI, Sayed AM (2005) Synthesis and characterization of tetra-functional epoxy resins from rosin. J Polym Res 12:127–138
30. Xie T, Rousseau IA (2009) Facile tailoring of thermal transition temperatures of epoxy shape memory polymers. Polymer 50:1852–1856
31. Ma SQ, Liu XQ, Fan L, Jiang Y, Cao L, Tang Z, Zhu J (2014) Synthesis and Properties of a bio-based epoxy resin with high epoxy value and low viscosity. Chemsuschem 7:555–562
32. Ma SQ, Liu XQ, Jiang YH, Tang ZB, Zhang CZ, Zhu J (2013) Bio-based epoxy resin from itaconic acid and its thermosets cured with anhydride and comonomers. Green Chem 15:245–254
33. Ma SQ, Liu WQ, Hu CH, Wang ZF, Tang CY (2010) Toughening of epoxy resin system using a novel dendritic polysiloxane. Macromol Res 18:392–398
34. Ma SQ, Liu WQ, Yu D, Wang ZF (2010) Modification of epoxy resin with polyether-grafted-polysiloxane and epoxy-miscible polysiloxane particles. Macromol Res 18:22–28
35. Chang R, Qin J, Gao J (2014) Retracted article: fully biobased epoxy from isosorbide diglycidyl ether cured by biobased curing agents with enhanced properties. J Polym Res 21:1–7
36. Bicu I, Mustata F (2007) Polymers from a levopimaric acid-acrylic acid Diels-Alder adduct: synthesis and characterization. J Polym Sci Part A Polym Chem 45:5979–5990
37. Wang H, Wang H, Zhou G (2011) Synthesis of rosin-based imidoamine-type curing agents and curing behavior with epoxy resin. Polym Int 60:557–563
38. Liu X, Xin W, Zhang J (2009) Rosin-based acid anhydrides as alternatives to petrochemical curing agents. Green Chem 11:1018–1025
39. Wei K, Zhu G, Tang Y, Tian G, Xie J (2012) Thermomechanical properties of shape-memory hydro-epoxy resin. Smart Mater Struct 21:55022–55029